CH-93-12-3

#6531

AIR VELOCITY CHARACTERISTICS IN AN EXPERIMENTAL LIVESTOCK BUILDING WITH NONISOTHERMAL JET VENTILATION

A.J. Heber, Ph.D., P.E. **C.R. Boon**
Member ASHRAE

ABSTRACT

Air velocity characteristics in a full-scale, climate-controlled section of a livestock building with a high ventilation rate were measured with three-dimensional ultrasonic anemometry, a new approach to indoor air velocity measurement. With simulated animal sensible heat of 160 W/m² (51 Btu/h per ft²) of floor, air jets projecting from both sides of a baffled diffuser under the peak of a gabled ceiling created nearly full, rotary air distribution patterns except for a small secondary circulation at the center of the room. Air turbulence was dominated by frequencies between 0.1 and 1.0 Hz and Eulerian length scales between 0.2 and 0.6 m (0.7 and 2.0 ft). Cross-sectional fields are presented for probability distributions of air velocity vectors and for various turbulence parameters including time and length scales, kinetic energy, energy dissipation, and microscale. A new definition for turbulence intensities and the use of irregularity factors are also introduced for describing turbulence fields in ventilated rooms.

INTRODUCTION

Proper distribution of air in a ventilated livestock building is essential to achieve satisfactory thermal conditions and air quality in both animal- and worker-occupied regions. Animals occupy the building 24 hours/day and workers up to 8 hours/day. In addition to mean air velocity and temperature, the turbulence intensity and frequency of air velocity fluctuations (especially around 0.4 Hz) have been shown to affect the thermal comfort of humans significantly (Fanger and Pedersen 1977; Melikov and Nielsen 1989; Thorshauge 1982). The effects of turbulence on the sensation of draft by animals and birds is unknown, but it directly affects indoor dispersion of gaseous and particulate pollutants that are harmful to both animals and workers. Thus a good understanding of air distribution patterns and turbulence characteristics of ventilation airflow in livestock buildings is needed.

Air movement in buildings is caused by nonlinear and variable external forces, such as the effects of heat and ventilation services and the operation/movement of equipment, animals, and people, and is therefore difficult to predict (Ljungqvist 1979). However, numerical simulations of room air have been developed to successfully predict velocity and turbulence in fields of two-dimensional, isothermal (Choi et al. 1990; El-Telbany et al. 1985; Nielsen et al. 1978) and nonisothermal (Chen et al. 1990) flow and three-dimensional, isothermal (Gosman et al. 1980; Haghighat et al. 1990) and nonisothermal (Awbi 1989) flow. Since a time series of air velocity can be analyzed in the frequency domain to determine spectral functions describing the structure of turbulence, energy transfer and dissipation can be quantified (Lay and Bragg 1988) and used to validate numerical simulations.

Several experimental studies have recently been conducted to measure air velocities and turbulence characteristics in model-scale isothermal (Murakami et al. 1988) and nonisothermal (Choi et al. 1909; Zhang et al. 1989) rooms, and full-scale nonisothermal rooms (Hanzawa et al. 1987; Melikov et al. 1990; Zhang et al. 1992). These experiments involved rooms with flat ceilings and wall-mounted diffusers. Detailed measurements of air velocity and turbulence characteristics have not been available for full-scale rooms with sloped ceilings or center-ceiling diffusers, a common configuration in agricultural buildings.

In previous studies, air velocities were usually measured with hot-wire anemometry, although laser-doppler anemometry was used by Gosman et al. (1980) and Nielsen et al. (1978). Although ultrasonic anemometry has the capability of measuring three-dimensional components of air velocity, it has not been used for studying air movement in ventilated rooms.

A.J. Heber is an associate professor, Agricultural Engineering Dept., Kansas State University, Manhattan, KS. **C.R. Boon** is a research scientist, Welfare Science Division, Silsoe Research Institute, Silsoe, Bedford, U.K.

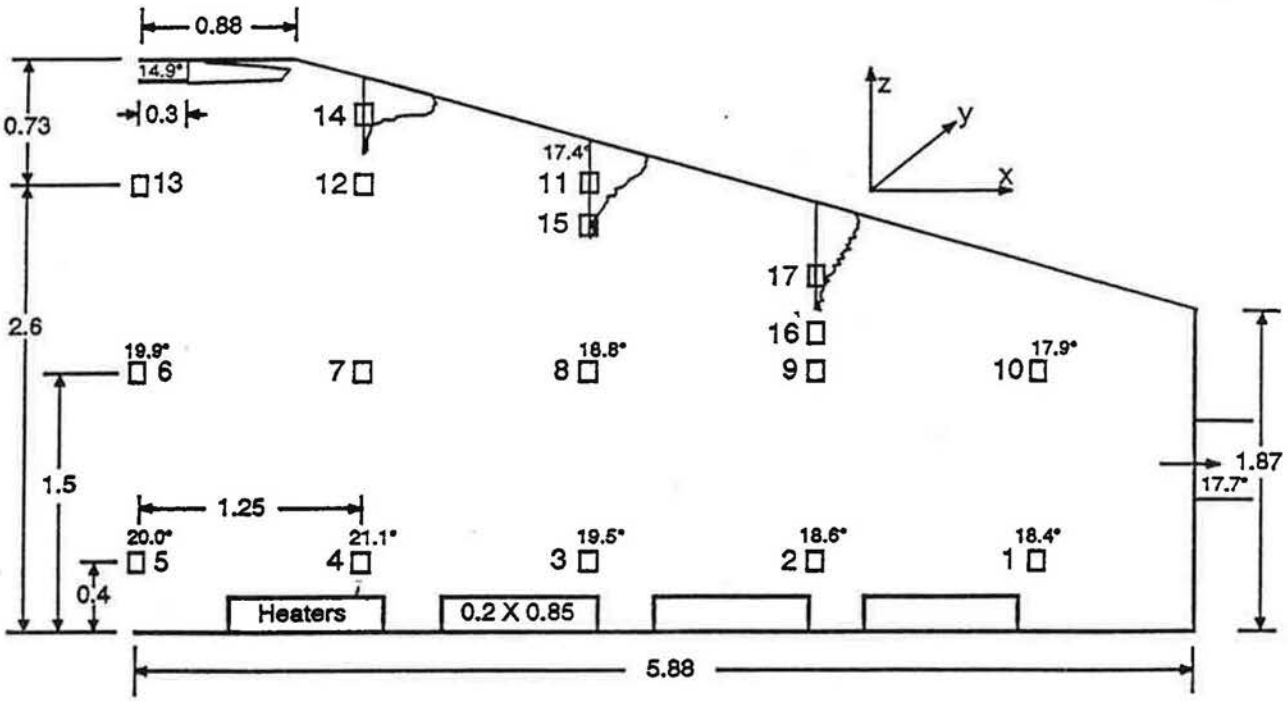

Figure 1 *Right half of building section showing sampling locations of sonic anemometer, inlet jet profiles, and average temperatures. All dimensions in meters and temperatures in degrees Celcius.*

The overall objective of the research reported in this paper was to evaluate turbulence characteristics and airflow patterns generated by a horizontal nonisothermal ventilation air jet in the special case of a full-scale livestock building section with a gable ceiling; a dual-sided, baffled, center-ceiling diffuser; and two sidewall exhaust fans. This ventilation system and building configuration is widely used for swine production in the United Kingdom and is described by Randall and Battams (1979). A relatively high ventilation rate to simulate warm weather conditions in a typical swine building was established along with the simulation of sensible heat produced by the swine. Air velocity and turbulence data at 17 cross-sectional positions are presented, and the effectiveness of a nonpoint ultrasonic anemometer for measuring air velocity in a livestock building under these conditions is evaluated. A new definition for turbulence intensities and the use of irregularity factors are also introduced for describing turbulence fields in ventilated rooms.

BACKGROUND

Air Velocity and Turbulence

The mean air velocity measured over a sampling period is

$$\bar{u} = \frac{1}{\Delta t} \int_{t}^{t+\Delta t} u \, dt \qquad (1)$$

whereas the instantaneous air velocity is

$$u = \bar{u} + u'. \qquad (2)$$

The variance of an air velocity record is defined as

$$\sigma^2 = u'^2 = \frac{1}{\Delta t} \int_{t}^{t+\Delta t} \left(u - \bar{u}\right)^2 dt. \qquad (3)$$

The standard deviation divided by local mean velocity is defined by others (Hanzawa et al. 1987) as turbulence intensity

$$\Psi = \frac{\sigma}{\bar{u}}. \qquad (4)$$

The integral of the energy spectrum, E(f), over all frequencies is the variance

$$\sigma^2 = \int_0^\infty E(f) \, df. \qquad (5)$$

The dispersive properties of turbulence depend on its energy and the distance over which the velocity fluctuations occur. These distances should be measured following the motion of the air, i.e., the Lagrangian length scales, but distances determined from fixed-point measurements, i.e., the Eulerian time scales, are more practical. The frequency

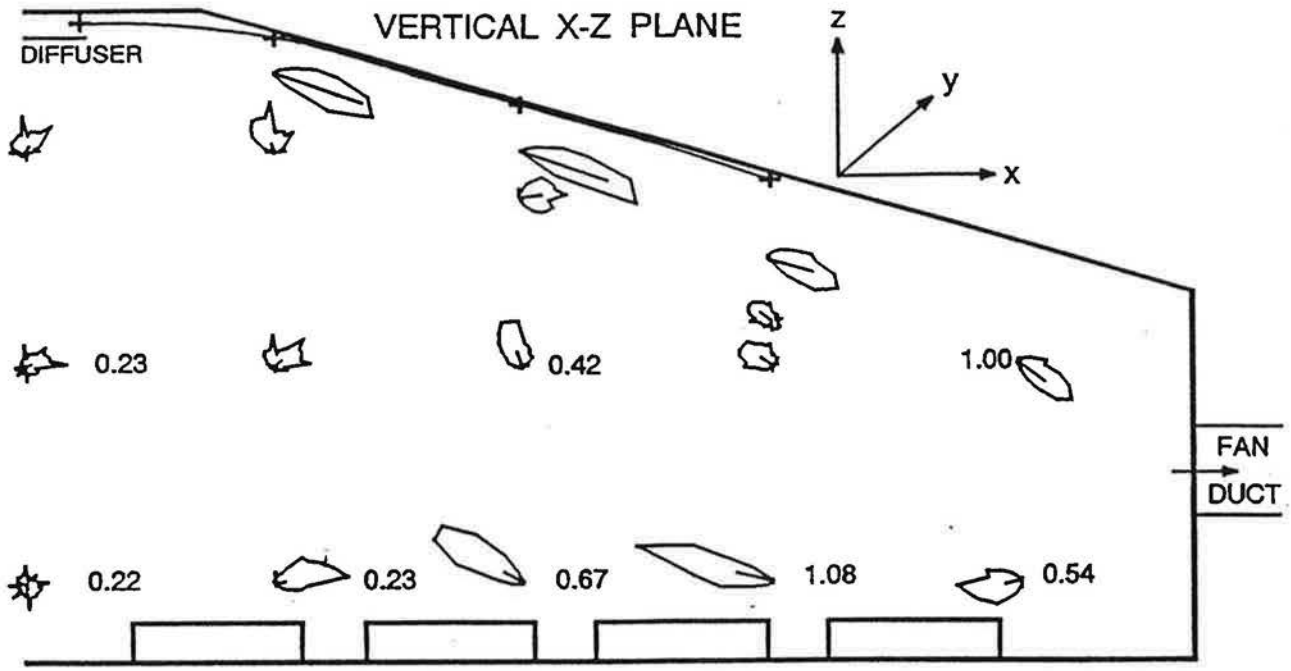

Figure 2 *Polar plots of probability densities of air flow direction in the z-x plane. Amplitude of u_x from the ultrasonic anemometer is shown as a line in approximate mean direction from each measurement point. The mean air speed (m/s) measured with a hot-wire probe is written at some locations. Locations of maximum jet velocities are marked with + symbol.*

responsible for most of the energy or variance (Equation 5) determines the turbulence time scale (Harrison and Perry 1977), which represents the largest eddies involved in the turbulent motion of the air (Hinze 1975). The characteristic frequency of these large eddies (Melikov et al. 1988) is

$$f_c = \frac{1}{2\pi T}. \qquad (6)$$

The normalized autocorrelation function, R(t), is the correlation between air velocities at a fixed location at two different instants, t' and t'+ t,

$$R(t) = \frac{u(t')\ u(t'+t)}{\sigma^2}. \qquad (7)$$

The Eulerian turbulence time scale was defined by Pasquill and Smith (1983) as the integral of R(t) over time lags from zero to infinity:

$$T_\theta = \int_0^\infty R(t)\ dt. \qquad (8)$$

An estimate of T_e is

$$\hat{T}_e = \frac{E(f)}{4\sigma^2} \text{ as } f \to 0, \qquad (9)$$

and the Eulerian turbulence length scale, representing the scale of mixing action, is

$$L_\theta = \bar{u} T_\theta. \qquad (10)$$

As opposed to integrating R(t) to infinity (Equation 8), we integrated only to the first zero crossing, t_0, to obtain what we denote as T_i, the "integral" time scale,

$$T_i = \int_0^{t_0} R(t)\ dt, \qquad (11)$$

and L_i, the "integral" length scale, also referred to as the macro scale (Hinze 1975),

$$L_i = \bar{u} T_i. \qquad (12)$$

Panofsky and Dutton (1984) defined a turbulence time scale as 1/f at the maximum fE(f):

$$T_m = \frac{1}{f_m}. \qquad (13)$$

The microscale of turbulence γ (Equation 14) represents the average size of the smaller eddies, which are mainly responsible for dissipation (Hinze 1975).

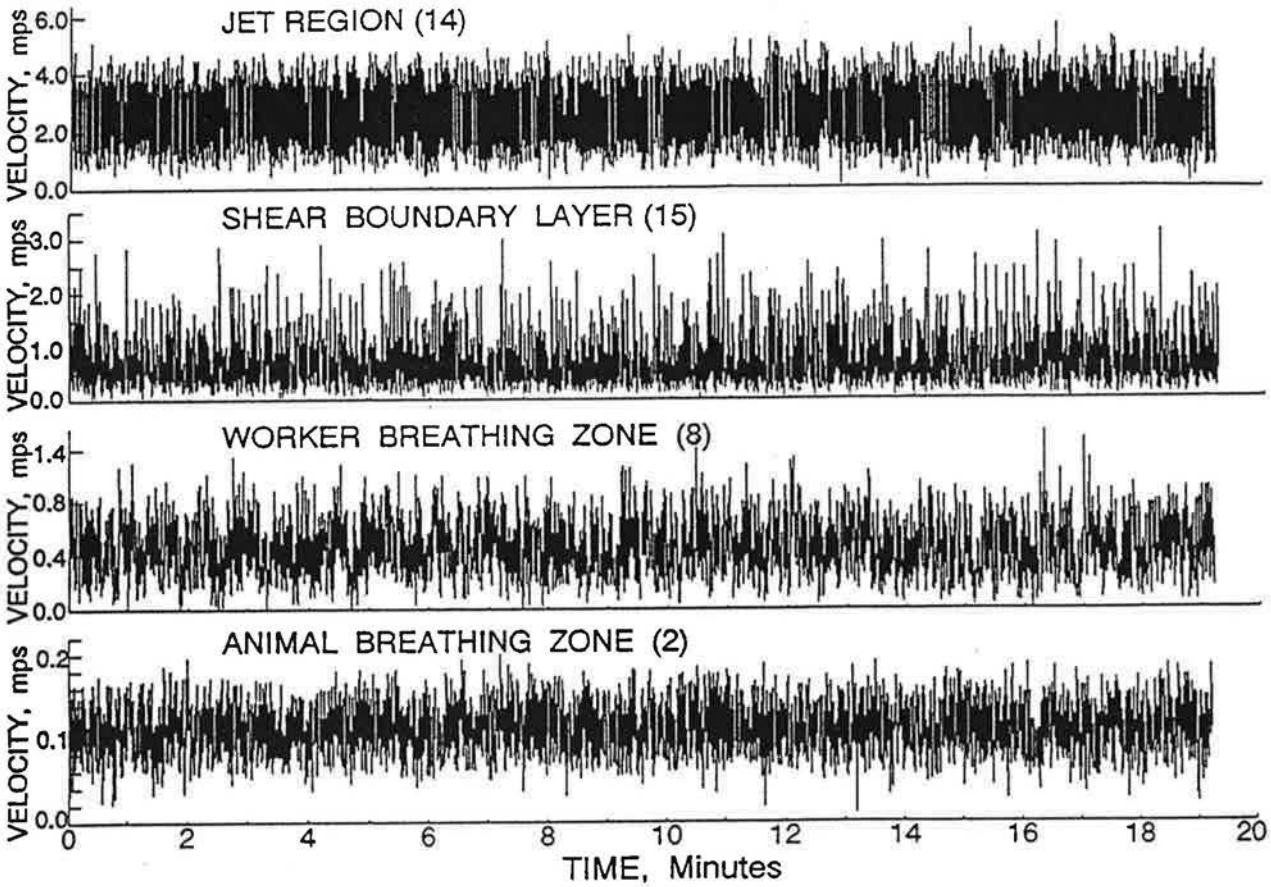

Figure 3 *Instantaneous amplitude of* u_u *at positions 2, 8, 14, and 15 (Figure 1) over a 19.25 minute sampling period.*

$$\lambda = \left[\frac{\bar{u}^2 \sigma^2}{2\pi^2 \int_0^\infty f^2 E(f)\, df} \right]^{\frac{1}{2}} . \qquad (14)$$

The total turbulence kinetic energy is calculated using Equation 15 (Pasquill and Smith 1983; El-Telbany et al. 1985):

$$k = \frac{1}{2}\left(\sigma_x^2 + \sigma_y^2 + \sigma_z^2\right) . \qquad (15)$$

The turbulence energy dissipation rate is

$$\epsilon = k^{\frac{3}{2}} \lambda^{-1} . \qquad (16)$$

The numerical simulations cited previously utilize transport equations of k and ε and are referred to as k-ε turbulence models.

Indoor Air Distribution

The size and position of the ventilation diffuser has a major effect on the flow pattern and air turbulence in a room (Awbi 1989; Jin and Ogilvie 1991b). Eddies in room air vary enormously in size, persistence, and translational and rotational velocity. Stable rotary flows cause floor air movement to be consistent with the primary rotary flow pattern (Jin and Ogilvie 1990). The energy in air turbulence arises from supply air jets, airstream obstructions, rough surfaces, localized convection currents, and mechanical motions within the room. The turbulence intensity is greater in jet ventilation systems than in displacement ventilation systems (Melikov et al. 1990).

Zhang et al. (1992) reported two-dimensional airflow measurements taken with a single-component hot-wire probe in a full-scale experimental room in terms of air velocity, turbulence kinetic energy, and temperatures. More turbulence and higher mean velocities occurred in the occupied space with nonisothermal jets as compared to isothermal jets. The turbulence in room ventilation flows were generated primarily by the air jet and secondarily by internal heat production.

Among 20 typical ventilated spaces evaluated by Hanzawa et al. (1987) with omnidirectional hot-wire probes, the mean velocity ranged from less than 0.05 m/s to 0.40 m/s (10 to 79 fpm) and turbulence intensity (Ψ) from 0.10 to 0.70. Energy

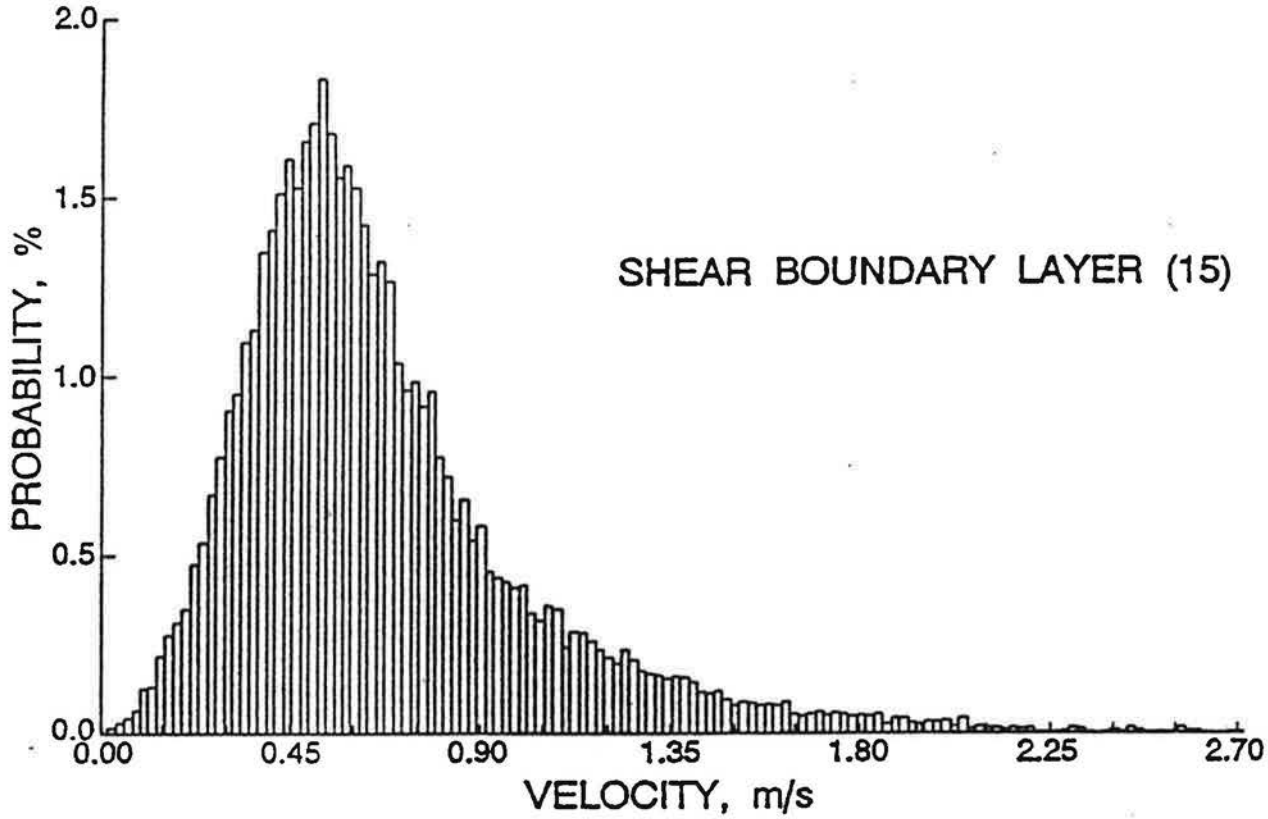

Figure 4 *Probability density distribution of u_u at position 15 (Fig. 1).*

spectra showed that most of the total turbulent energy was due to large eddies. The mean air speed in the animal occupation zone in a swine building was about 0.15 m/s (30 fpm) with natural convection and 0.63 m/s at the maximum, fan-powered ventilation rate (Boon 1982).

Air Movement and Contaminant Dispersion

The velocity field and turbulence fields are of fundamental importance in contaminant dispersion by room ventilation (Siurna and Bragg 1986). In slow-moving air with u<0.30 m/s (59 fpm) or in laminar flow, gases moving by molecular diffusion travel considerably faster than particles (less than 7 μm [2.8 x 10^{-4} in.] diameter) moving by Brownian diffusion. The mechanisms by which airborne contaminants move because of turbulence are complex and consist of a combination of effects. According to Ljungqvist (1979), turbulence created in a room—even at low air speeds with u = 0.20 m/s (40 fpm)—was the predominant factor in the diffusion of both gases and particles. Turbulence transports airborne matter in relatively large agglomerations and eliminates the difference in diffusion coefficients between gases and particles.

Ljungqvist (1979) reported that in a 3 x 3 x 3 m (9.8 x 9.8 x 9.8 ft) room with a slotted ventilation diffuser, a consistent room-size vortex could not be established at air exchange rates less than 10 to 15 air changes per hour (ach) even in isothermal conditions. At air exchange rates less than 10 ach, airflow patterns were easily disrupted by very small thermal disturbances, whereas stabilization occurred with reproducible velocity fields at airflow rates above 15 ach. Airflow at 20 ach was characterized by high levels of turbulence even at the center of the room-size vortex and, at 40 ach, this turbulence became isotropic. Room vortices were characterized by "flash-like" turbulence and rotated as a rigid body, with closed streamlines becoming circular and velocity increasing linearly from the center.

PROCEDURE

The experiments were conducted in a building section that was designed to study ventilation airflow patterns. This section is similar in concept to the section described by Boon (1978), the main difference being that it is not capable of housing live animals. The structure is a cross section of a typical U.K. intensive livestock building, representing one

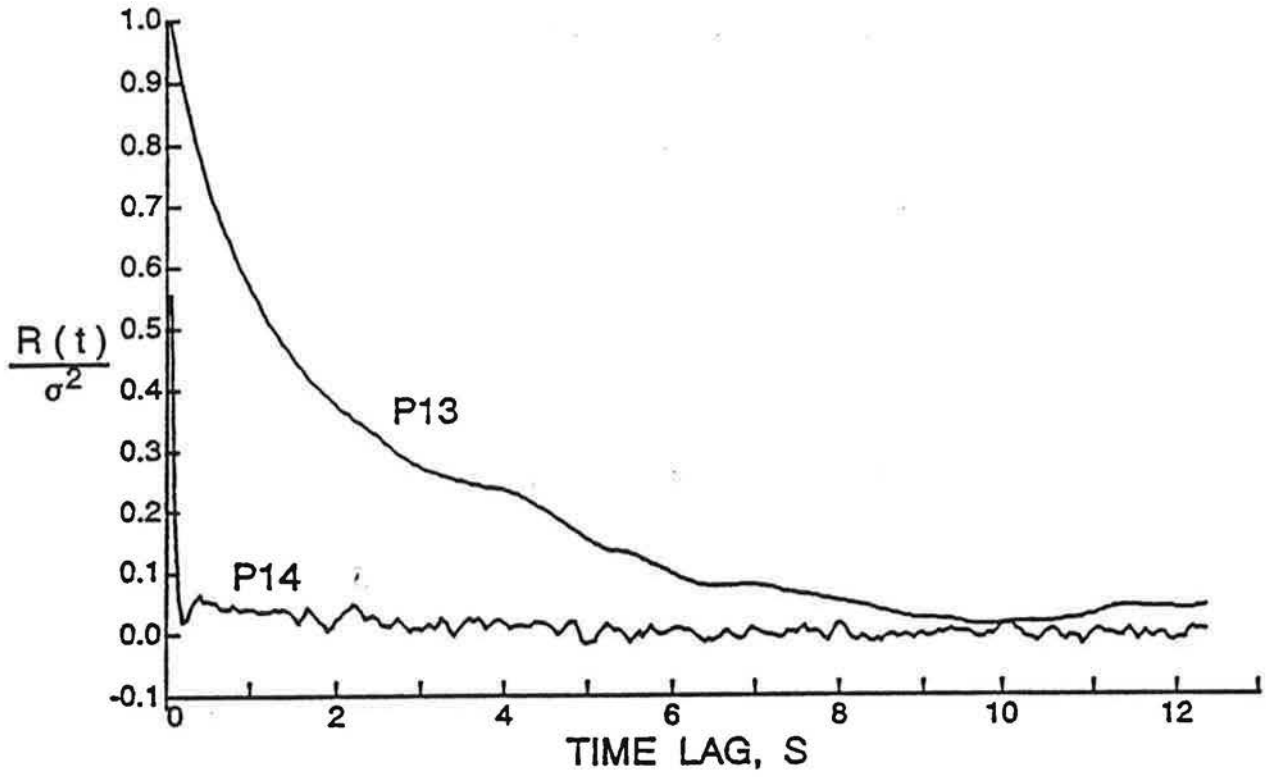

Figure 5 *Normalized auto correlation function for u_u at position 13 and 14 (Fig. 1).*

bay of 3 m (9.8 ft) length and containing two pens separated by a 1.0 m (3.3 ft) wide central feeding passage. The section is 11.7 m (38.4 ft) wide with a 14.5° ceiling slope, 3.34 m (11 ft) to the ridge and 1.88 m (6.2 ft) to the eaves, and its insulation characteristics are similar to those of a standard building (Figure 1). The front of the section is glass to facilitate airflow visualization. The room is ventilated by a jet ventilation system. The air enters horizontally in each direction from a 142 x 982 mm (5.6 x 38.8 in.) baffled ceiling diffuser at the ridge. The baffle directs the air horizontally just below the peak of the ceiling toward the building sidewalls. A 450 mm (17.7 in.) diameter exhaust fan is mounted at the end of a 0.8-m duct inserted flush in each sidewall. The centerline of the fan duct is 0.96 m (37.8 in.) above the floor and 85 cm from the rear wall. Fan airflow rate was measured by a traverse of air velocities through each fan duct. The room is surrounded by an temperature-controlled outer shell (5°-25°C [41° to 77°F]) and, thus, precise ambient temperature can be established.

The simulation of sensible heat output of livestock was achieved by 160 resistance element heater strips measuring 115 x 615 mm (4.5 x 24 in.) and 160 strips measuring 75 x 615 mm (3 x 24 in.) hung vertically in wooden racks. Eight racks, each with 20 wide heater strips, and eight racks, each with 20 narrow heater strips, were arranged symmetrically on the floor to provide relatively uniform convection currents from the animal lying zones (Figure 1).

Temperatures, ventilation rates, fan static pressure, and air speeds were also monitored. Temperatures were measured at positions 1 through 16 (Figure 1) using copper-constantan thermocouples. Air speed was measured at positions 1 through 5, 6, 8, and 10 using heated thermocouple anemometers. Two of these were also used to measure ventilation rate. Air velocity profiles in the jet were measured by manually traversing vertically with a hand-held, omnidirectional, hot-wire probe. It was necessary for a person to be present in the room only for these measurements, which were conducted separately from the recorded measurements of the other instruments.

An ultrasonic anemometer was used at 17 positions distributed throughout the right-hand half of the section (Figure 1). The anemometer used a 110 x 110 x 100 mm (4.3 x 4.3 x 3.9 in.) measurement "volume" to attain a 150-mm (5.9-in.) sound travel distance between three transmitter/receiver sets. The instantaneous and 10-second average horizontal air speed accuracies (with the instrument in the vertical position) were given by the manufacturer as ±3 and ±1%, respectively. At each position, the 0.75 m (29.5 in.) long instrument was positioned vertically downward for positions 1 through 5 (Figure 1) and vertically upward at other positions. The positive x-direction was from the building center to the right-hand-sidewall, the y-direction was along the center line to the rear end wall, and the z-direction was vertically upward from the floor.

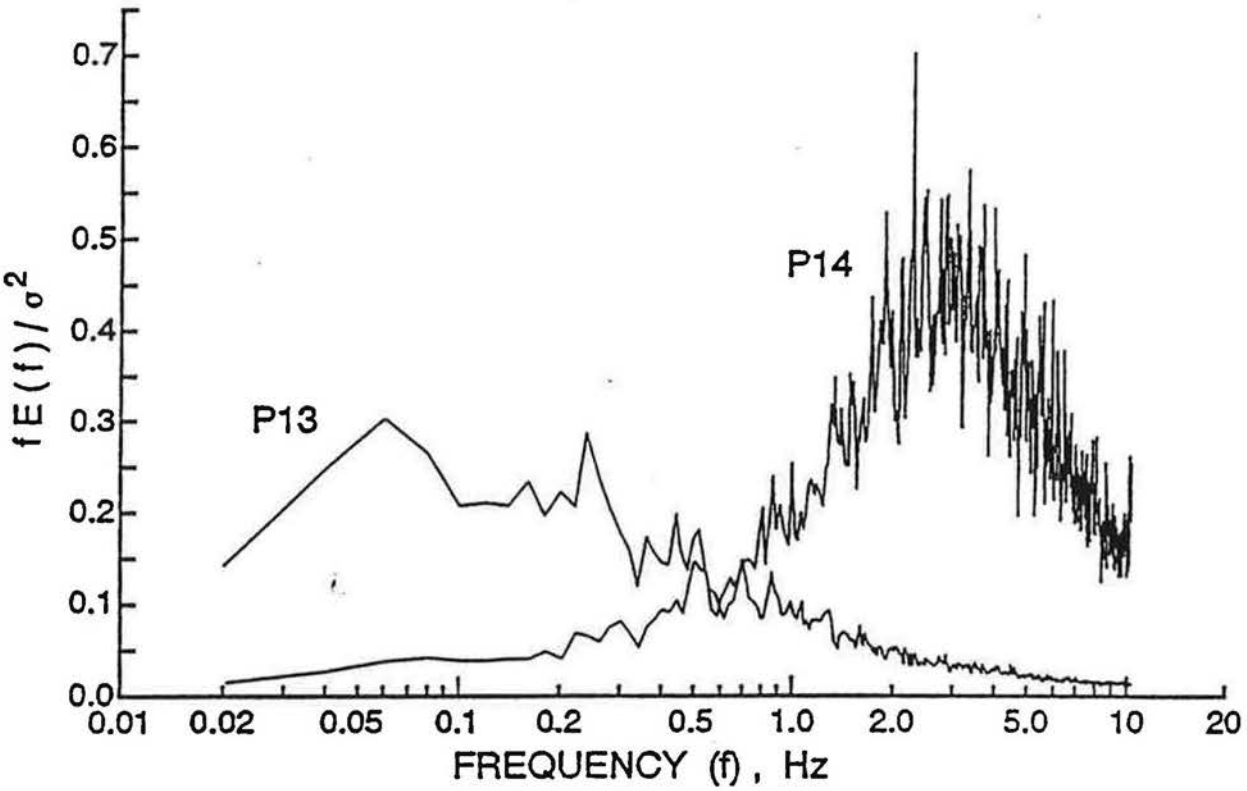

Figure 6 *Normalized spectra for u_u at positions 13 and 14 (Fig. 1).*

Table 1
Analysis of air velocity data from the ultrasonic anemometer

Pos	Mean		Skew	Max		Ψ	Ψ_r	ι	k		T_e	T_o	T_i	T_m	$\mathcal{L}_o$		L_i		λ		ϵ		f_c
																					$(x10^{-3})$		
	m/s	ft/min		m/s	ft/min				m^2/s^2	ft^2/min^2	s	s	s	s	m	ft	m	ft	m	ft	m^2/s^3	ft^2/min^3	Hz
1	0.76	150	0.04	1.59	313	0.26	0.026	0.41	0.059	2285	0.90	0.80	0.75	2.35	0.608	1.99	0.570	1.87	0.117	0.38	0.12	285	0.21
2	1.11	218	0.00	2.02	398	0.22	0.033	0.49	0.095	3679	0.44	0.35	0.33	2.24	0.389	1.27	0.364	1.19	0.137	0.45	0.21	497	0.48
3	0.56	110	0.74	1.62	319	0.39	0.029	0.38	0.051	1956	0.89	0.74	0.89	2.24	0.414	1.36	0.496	1.63	0.115	0.38	0.10	229	0.18
4	0.29	57	0.63	0.86	169	0.41	0.016	0.32	0.020	775	2.22	2.06	2.22	12.32	0.597	1.96	0.633	2.08	0.063	0.21	0.04	104	0.07
5	0.25	49	0.67	0.84	165	0.50	0.017	0.31	0.038	1472	2.20	2.14	2.20	7.04	0.535	1.75	0.567	1.86	0.057	0.19	0.13	300	0.07
6	0.26	51	0.60	0.88	173	0.48	0.017	0.29	0.039	1510	2.00	2.26	2.00	9.86	0.588	1.93	0.506	1.66	0.060	0.20	0.13	298	0.08
7	0.24	47	1.01	1.06	209	0.53	0.017	0.30	0.029	1123	1.59	1.50	1.59	4.93	0.360	1.18	0.367	1.21	0.059	0.19	0.08	195	0.10
8	0.46	91	0.34	1.33	262	0.40	0.025	0.42	0.059	2285	0.69	0.71	0.66	3.52	0.327	1.07	0.304	1.00	0.076	0.25	0.19	439	0.24
9	0.37	73	0.75	1.38	272	0.47	0.023	0.36	0.066	2537	0.76	0.53	0.76	3.29	0.196	0.64	0.275	0.90	0.071	0.23	0.24	546	0.21
10	0.89	175	0.86	3.31	651	0.52	0.062	0.46	0.272	10535	0.46	0.40	0.34	1.54	0.356	1.17	0.308	1.01	0.134	0.44	1.06	2458	0.46
11	2.36	464	0.28	5.39	1061	0.33	0.104	0.66	0.591	22890	0.18	0.16	0.18	0.67	0.378	1.24	0.420	1.38	0.196	0.64	2.32	5389	0.90
12	0.25	49	0.76	0.81	159	0.50	0.017	0.42	0.026	1007	1.15	1.11	1.15	4.93	0.278	0.91	0.298	0.98	0.047	0.16	0.09	206	0.14
13	0.26	51	0.41	0.88	173	0.49	0.017	0.25	0.029	1123	2.05	2.24	2.04	16.43	0.582	1.91	0.528	1.73	0.066	0.22	0.08	175	0.08
14	2.42	476	0.26	5.64	1110	0.31	0.100	0.75	0.615	23800	0.15	0.16	0.13	0.44	0.387	1.27	0.319	1.05	0.147	0.48	3.27	7599	1.21
15	0.67	132	1.62	3.14	618	0.53	0.047	0.58	0.175	6758	0.26	0.21	0.26	0.91	0.141	0.46	0.175	0.57	0.078	0.26	0.94	2177	0.60
16	0.56	110	0.73	2.17	427	0.45	0.034	0.44	0.133	5151	0.51	0.46	0.51	1.97	0.258	0.84	0.287	0.94	0.085	0.28	0.57	1329	0.31
17	1.30	256	0.73	3.95	777	0.45	0.078	0.53	0.412	15937	0.29	0.25	0.25	1.41	0.325	1.07	0.367	1.21	0.160	0.53	1.65	3824	0.65
Avg	0.77	151	0.61	2.17	427	0.43	0.039	0.43	0.159	6166	0.98	0.95	0.96	4.47	0.395	1.30	0.399	1.31	0.098	0.32	0.66	1532	0.35
Analysis of differences between two separate tests for positions P1-P13.																							
$\bar{\Delta}^*$	-0.02	-4.7	0.00	-0.11	-23	-0.01	0.001	0.00	-0.003	-134	0.17	0.18	0.19	0.21	0.090	0.30	0.079	0.26	0.000	0.00	-0.01	-29	0.07
e^{**}	0.05	10	0.11	0.06	6.8	0.02	0.001	0.01	0.005	199	0.09	0.10	0.09	0.86	0.054	0.18	0.058	0.19	0.007	0.02	0.02	34	0.08

*Mean difference (n=13)

**Standard error of mean

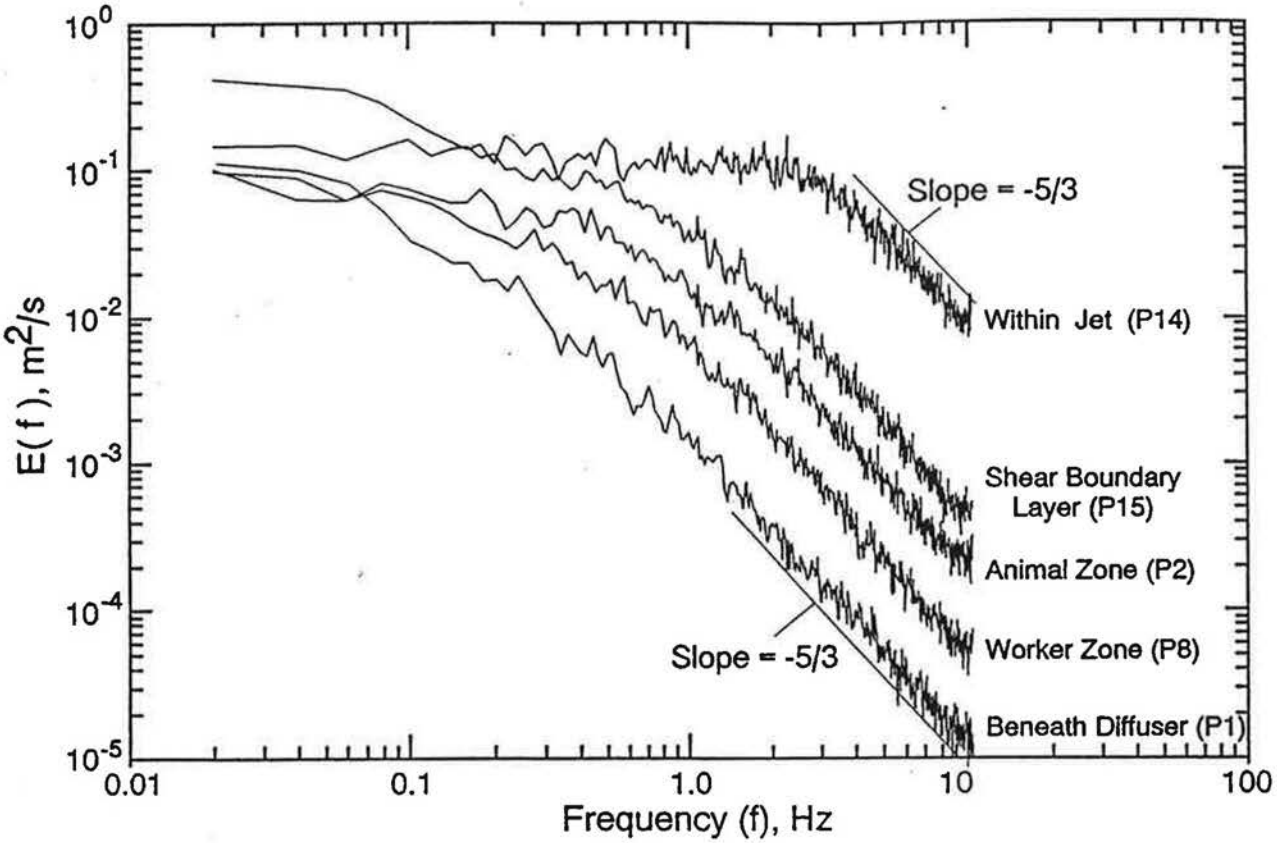

Figure 7 *Spectral distribution of u_u at positions 2, 8, 13, 14, and 15 (Fig. 1).*

Each experimental run consisted of a 19.25-min data acquisition from the anemometer, which gave 24,000 values at a 20.78-Hz sampling rate for each of the x, y, and z directions. This time was needed to attain a statistically significant number of ensembles for Fourier analysis. A commercial software package was used for spectral analysis of the velocity records from the ultrasonic anemometer. Energy spectra and correlation functions were smoothed by averaging ensembles of 24.6 seconds in duration, close to the 30 seconds minimum sampling time recommended by Jin and Ogilvie (1990).

Measurements with the anemometer at positions 1 through 13 were repeated in another test with attempted identical experimental conditions. The mean and standard errors of the differences of all parameters between the first and second tests were calculated to evaluate the repeatability of the experimental measurements.

Two variables not mentioned in the literature are used in this paper to describe the turbulence fields in the building. The first involves a slight redefinition of turbulence intensity. The conventional definition of turbulence intensity, Ψ (Equation 4), is useful for comparing the turbulence of air at similar mean velocities: however, it loses meaning when describing a turbulence field with widely varying mean velocities, and at low and unstable room air velocities where the mean air velocity approaches zero, resulting in very large values of Ψ. For three-dimensional resultant velocities of room air, u_u, it is proposed that the maximum diffuser velocity, u_{uim}, be used to define turbulence intensity in a room as

$$\Psi_r = \sigma / \bar{u}_{udm} \qquad (17)$$

The advantages of Ψ_r are that it: (1) does not depend on the local mean velocity, (2) is proportional to the square root of the turbulence kinetic energy, (3) is useful for comparing relative turbulence in an air space with widely varying mean velocities, and (4) is referenced to the maximum mean air velocity in the air space where turbulence intensity is also expected to be the highest.

The second new variable for describing the turbulence field is the irregularity factor, ι. The irregularity factor, ι, of a time series is defined as the total number of mean crossings divided by the total number of peaks between mean crossings. The irregularity factor of a perfect sine wave is 1.0. Its advantage over Ψ and Ψ_r in describing the turbulence field in a room is its independence of mean air velocity.

RESULTS AND DISCUSSION

The fan operating characteristics were kept constant for all runs as the ultrasonic anemometer was moved from one location to the next. The average fan static pressure and speed were 39 Pa (0.16 in. H_2O) and 1,085 rpm, respectively. The average airflow rate was 0.84 m^3/s (1,779 cfm) per fan or 1.67 m^3/s (3,536 cfm) for the room or 62.9 air changes per hour (ach). An exchange rate of 60 ach was recommended by Jin and Ogilvie (1991b) as a maximum practical ventilation rate for a swine shelter under hot weather conditions.

The total simulated heat output was 5.65 kW (19,299 Btu/h) based on heat balance calculations. This is equivalent to the sensible heat output of 55 90-kg pigs at 19.5°C (67°F), the average temperature in the animal occupation zone. The space allocation for these pigs would be 0.58 m^2 (6.24 ft^2) per head, as compared to United Kingdom and United States guidelines of 0.50 and 0.75 m^2 (5.4 and 8.0 ft^2) per head, respectively; the ventilation rate would be 0.030 m^3/s (64.3 cfm) per pig, as compared to recommended warm and hot weather ventilation rates of 0.028 and 0.057 m^3/s (60 and 120 cfm) per pig (Bodman 1991).

The diffuser jet momentum number, J, which is used as a basis for diffuser baffle control (Albright 1989), was 1.7 x 10^{-2}. Barber and Ogilvie (1982) and Leonard and McQuitty (1988) have proposed minimum criteria of $J = 7.5 \times 10^{-4}$ and $J = 20 \times 10^{-4}$, respectively, for optimum mixing under nonisothermal conditions in cold weather.

The Archimedes number (Ar) is the ratio of buoyancy to inertial forces on the air jet and is used to characterize the trajectory of ventilating air jets. The corrected Archimedes number, $Ar_{corr} = (HW/D_r^2)Ar$, accounts for various diffuser proportions (Randall and Battams 1979). The jet remains horizontal after entry if $Ar_{corr}<40$. The corrected Archimedes number for this jet was 5×10^{-5}. Using the average diffuser face velocity of 6.03 m/s (1,187 fpm), the diffuser Reynolds number was 90,083 based on the diffuser hydraulic diameter, $D_d = 0.247$ m (0.81 ft), and 51,633 based on the diffuser height, W = 0.1415 m (0.464 ft).

The average temperatures of incoming and exhaust (fan) air, and the surface temperature of the heaters were 14.9°, 17.7°, and 27.7°C (58.8°, 63.9°, and 91.9°F), respectively (Figure 1). Incomplete mixing as theorized by Barber and Ogilvie (1982) was evident, as a 2.6°C (4.7°F) temperature gradient was established in the animal occupation zone near the floor from the sidewall toward the center passageway. Similarly, a 2°C (3.6°F) temperature gradient occurred in the worker breathing zone.

Air Velocities

The jet velocity profiles are superimposed on the cross section of the building in Figure 1. The maximum jet velocity was 7.5 m/s (1,476 fpm) at the diffuser and decayed to 5.6, 4.4, and 3.3 m/s (1,102, 866, and 649 fpm) at horizontal distances of 0.95, 2.20, and 3.45 m (3.1, 7.2, and 11.3 ft) from the diffuser, respectively. The points of maximum velocity in the jet are connected by a line in Figure 2. Sampling positions 11 and 14 were somewhat immersed in the jet but at significantly lower heights than the maximum jet velocity (Figure 1). Sampling position 15 (P15) was located in the reentrainment boundary of the jet.

The three-dimensional resultant air velocity, $\bar{u}_a$, ranged from 0.24 m/s (47.2 fpm) at P7 to 2.42 m/s (476 fpm) at P14 (Table 1). Reasonable stationarity of mean and variance of air velocity was achieved at each measurement point. For example, during the first, second, and third successive sets of 8,000 data points at P1, the mean velocities were 0.78, 0.77, and 0.74 m/s (153.5, 151.5, and 145.6 ft/min) and the standard deviations were 0.21, 0.18, and 0.21 m/s (41.3, 35.4, and 41.3 ft/min), respectively. The mean difference between the ultrasonic anemometer and the hot-wire probe measurements at P1 through P6, P8, and P10 in Figure 2 was 0.02 m/s (4.7 fpm), with a standard error of 0.03 m/s (6.8 fpm).

The maximum instantaneous u_u was 5.6 m/s (1,102 fpm) at P14 in the jet region. The increased frequency of velocity fluctuations with height above the floor was evident in the air velocity records at P2, P8, P15, and P14 (Figure 3). The probability density distribution at P15, where the ultrasonic anemometer was immersed in the shear layer boundary of the wall jet, was non-Gaussian (Figure 4). The air velocity, u_u, at P15 was characterized by a high level of intermittency, as indicated by a large skew to the right of 1.62 and a kurtosis of 7.0 (Table 1). On the other extreme, a skew of 0.0 and a kurtosis of 3.0 were calculated for u_u at P2, indicating a perfectly Gaussian distribution. Skew and kurtosis of all the velocity records averaged 0.6 and 3.5, respectively, indicating non-Gaussian distribution in some parts of the room, particularly in the shear boundary layer. A function of the gamma family, particularly the chi-square function, would better describe the distribution. Zhang et al. (1991) also noted that the probability density function of room air velocity fluctuations were slightly right skewed, but concluded that Gaussian distribution was a reasonable approximation for practical application.

The probability densities of airflow direction in thevertical plane (x-z axes) are shown as polar plots (similar to meteorological wind roses) at each position in Figure 2. The measurement position was used as the origin of each plot, and the frequencies of direction in 10° intervals are connected by a line. These polar plots were characterized by peaks at the 45°points at those positions with very low mean velocities ($u_v < 0.03$ m/s [6 fpm]) because of the 0.01-m/s (2-fpm) resolution per each three-dimensional component of the ultrasonic anemometer. The relative amplitudes of u_v are plotted as lines for all positions in Figure 2. These lines were oriented in the approximate mean direction of airflow, which was somewhat vague at positions such as P5, where the flow was quite unstable.

The polar plots in Figure 2 show that the airflow pattern was characterized by the stable primary vortex rotating clockwise in the right two-thirds of the half-section and an unstable secondary vortex rotating counterclockwise at the lower center of the room. The most stagnant area was in the passageway near the floor (P5), followed by the worker

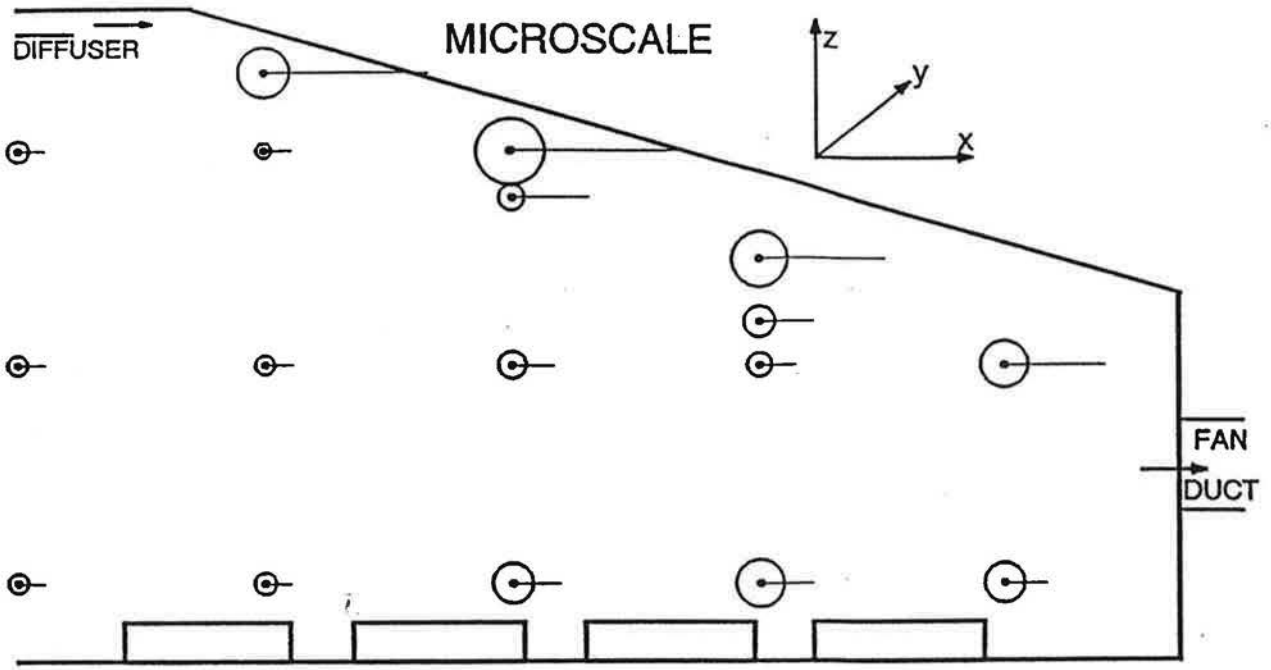

Figure 8 *Relative size of turbulence mecroscale γ(circles) for U_u at each measurement location. The microscale was 0.196 m at position 11 and 0.047 m at position 12 (see Fig. 1). Horizontal lines represent the relative value of turbulence intensity Ψ_r.*

breathing zone (P6). A relatively strong upward movement of air occurred between P3 and P4 and between P7 and P8 and was apparently aided by heater-generated convection currents. This air pattern was described by Jin and Ogilvie (1990) as a "stage 3" flow pattern, which occurs when the diffuser jet momentum is too small to establish fully rotary and stable flow (stage 4) in the room.

The two-dimensional air velocities u_h in the horizontal plane (x-y), u_h, and in the transverse plane (z-y), u_t, indicated that some transverse airflow occurred in the building section, with air tending to flow toward the back wall at P1 and P2 and toward the front wall at P4, P8, P15, and P16. This can be partially attributed to the asymmetrical location of the fan, which was nearer the back wall than the front wall.

Turbulence Characteristics

Several parameters describing the turbulence of u_u were calculated. The turbulence intensity, Ψ_r (Equation 17), ranged from 0.016 at P4 to 0.104 at P11 and is mapped on the room cross section in Figure 8. The level of turbulence intensity decreased with jet travel distance or air parcel residence time in the room and was greater in the primary vortex than in the secondary vortex (positions P4 through P7, P12, P13). The same distinct pattern also occurred with the irregularity factor, ι_u, which ranged from 0.25 at P13 to 0.75 at P14, and turbulence kinetic energy, k, which ranged from 0.02 m^2/s^2 (775 ft^2/min^2) at P4 to 0.62 m^2/s^2 (23,800 ft^2/min^2) at P14 (Table 1).

The normalized autocorrelation functions, R(t), at P13 and P14 (extremely high and low, respectively) are shown in Figure 5. The R(t) at P14 became negative at a 3.5-second time lag, thus t_o=3.5 in Equation 11. The R(t) at P13 was positive up to the time lag limit of 12.3 seconds or 50% of the 24.6 second ensemble period, thus t_o = 12.3. The Eulerian and integral time scales determined from integrating R(t) versus time lag (Equations 8 and 11) ranged from about 0.15 seconds at P14 to about 2.15 seconds at P4, P5, P6, and P13 (Table 1). The integral length scales ranged from 0.18 m (0.59 ft) at P15 to 0.57 m (1.87 ft) at P1. The turbulence time and length scales consistently increased with jet travel distance (Table 1).

The average integral length scale of 0.40 m (1.3 ft) was on the same order of magnitude as the three 0.15-m (0.49-ft) sound path lengths of the ultrasonic anemometer. This leads to greater uncertainties in the determination of the turbulence length scales with ultrasonic anemometry than with those measured by "point" sensors such as hot-wire anemometers, especially in the more turbulent regions of the room.

The dominant frequencies in the turbulence energy are given by the fE(f) spectra (Figure 6). The frequency at which the maximum peak occurred was used to calculate T_m (Equation 13), which averaged about 4.5 times larger than T_e (Table 1). According to Panofsky and Dutton (1984), T_m is usually four to six times larger than T_e. The maximums of the fE(f) spectra were not always clearcut and may also represent a very narrow range of frequency indicated by very

sharp peaks. This results in greater uncertainty with this time scale than with T_e and T_i.

The energy spectra at P2, P8, P13, P14, and P15 (Figure 7), show that less turbulence energy was associated with high frequency at greater jet travel distances. The jet was the most turbulent, followed by the shear boundary layer where room air is entrained into the jet. The air in the animal zone contained more turbulence energy than in the worker breathing zone due to the turbulent jet along the ceiling turning around at the sidewall and behaving as an air jet along the floor in the reverse direction. With the high airflow rate used in this experiment, the "wall" jet was able to stay attached to the boundaries (ceiling, wall, floor) until it reached position P3, where it was finally overcome by the force of rising convection currents. For this reason, the maximum air velocities and turbulence energy are near the boundaries, and less turbulence energy occurs in the worker breathing zone, which is farthest from any boundary. Finally, the relatively stagnant secondary vortex contained the least turbulence energy, especially just beneath the ventilation diffuser at position P13.

The decay rate of the energy density of isotropic turbulence at high frequencies is $f^{-5/3}$ (Hinze 1975). Though the sampling rate was slow relative to jet turbulence, it was sufficient to establish the -5/3 slope of the inertial subrange (Figure 7) allowing one to extrapolate to find the energy density at higher frequencies.

The E(f) used to calculate $\hat{T}_e$ in Equation 9 was taken at the smallest frequency. This is a good approximation of E(0) because the curves become relatively horizontal at low frequencies, i.e., $E(f) \approx 0.1$ as $f \rightarrow 0$ for P8 and P13 (Figure 7). The values of T_e and $\hat{T}_e$ were nearly equivalent (Table 1).

The characteristic frequency (Equation 13), was at least 15 times larger in the jet region (f_c = 1.2 Hz) than in the secondary vortex at the center of the room's cross section (f_c = 0.07 Hz). It ranged from 0.07 to 0.48 Hz in the animal and worker breathing zones (positions P1 through P10), agreeing with the 0.4 Hz detected by Jin and Ogilvie (1991a) in empty rooms.

The microscale of turbulence ranged from 0.05 m (0.16 ft) at P12 to 0.20 m (0.66 ft) at P11 and is plotted as circles in Figure 8. The microscales were largest in the primary room vortex and decreased as the air flowed from P14 to P3 and upward to P8, P9, and P16. A similar pattern was observed with u_a (Figure 2), to which the microscale was linearly related with an $R^2 = 0.79$.

The turbulence energy dissipation, ε, ranged from 0.04 m^2/s^3 (104 ft^2/min^3) at P4 to 3.3 m^2/s^3 (7600 ft^2/min^3) at P14 (Table 1), and showed the same pattern as γ except for larger values at P15, P16, P8, and P9 in relation to those at P1, P2, and P3.

The irregularity factor, ι, averaged 0.43 and ranged from 0.25 at P13 to 0.75 at P14. It decreased by a factor of three as air traveled from the turbulent jet at the diffuser to the relatively stagnant area beneath the diffuser.

Comparison with a Repeat Test

The comparison of results with an identical test conducted several months later is shown in Table 1 for positions P1 through P13. Generally, the mean differences (second test value - first test value) were less than 5% of the average for values directly related to the mean and variance of air velocity and 15% to 30% for parameters derived from spectral analysis of the velocity record. The largest differences occurred at positions P2, P3, and P4, where the local air movement was very sensitive to the position of the heaters, which may inadvertently have been slightly repositioned before the repeat test. Repeatability was best at greater heights above the floor (P8 through P12).

CONCLUSIONS

1. Full rotary motion was nearly achieved except that a small, unstable secondary vortex formed in the lower center of the room (Figure 2).

2. The dominant frequency of air turbulence was about 15 times greater in the jet 2.2 m (7.2 ft) from the diffuser than in the secondary vortex.

3. Turbulence time and length scales increased, whereas the irregularity factor, characteristic frequency, kinetic energy, energy dissipation, and microscale decreased with jet travel distance around the cross-sectional flow pattern.

4. Significant transverse vortices existed in the building section.

5. The distribution of air velocities was non-Gaussian at some positions in the room, especially in the shear boundary layer of the jet, because the skew of air velocity ranged from 0 to 1.6 and kurtosis ranged from 2.6 and 7.0.

6. The ultrasonic anemometer had the range, accuracy, and portability appropriate for measuring air velocities (speed and direction) inside livestock buildings with high ventilation rates. The 20.78-Hz sampling rate was satisfactory for the occupied zone but was low for turbulence in the jet region.

7. Greater uncertainties in the determination of the turbulence length scales can be expected with ultrasonic anemometry than with hot-wire anemometry since the turbulence length scales were only slightly larger than the sound path lengths of the ultrasonic anemometer.

ACKNOWLEDGMENTS

Cooperative support for this work was received from the Agriculture and Food Research Council's Silsoe Research Institute and the Kansas Agricultural Experiment Station (Contribution No. 92-432-J). Technical advice and assis-

tance from B.J. Legg, P.J. Walklate, R.P. Hoxey, B.B. Harral, M.R. Holden, and others are much appreciated.

NOMENCLATURE

D	=	hydraulic diameter, m
E	=	spectral density, m^2/s
H	=	vertical height of ventilation diffuser, m
L	=	turbulence length scale, m
R	=	normalized autocorrelation function, m^2/s^2
T	=	turbulence time scale, s
W	=	horizontal width of ventilation diffuser, m
f	=	frequency, s^{-1}
q	=	turbulence kinetic energy, m^2/s^2
t	=	time, s
u	=	air velocity, m/s
$\bar{u}$	=	time-mean value of air velocity, m/s
Ψ	=	turbulence intensity
γ	=	microscale, m
σ	=	standard deviation, m
ε	=	turbulence energy dissipation rate, m^2/s^3
ι	=	irregularity factor

Subscripts

x	=	horizontal direction, positive left to right
y	=	horizontal direction, positive front to back
z	=	vertical direction, positive upward
t	=	two-dimensional vertical resultant in y-z plane
v	=	two-dimensional vertical resultant in x-z plane
h	=	two-dimensional horizontal resultant in x-y plane
u	=	three-dimensional resultant in x-y-z plane
c	=	characteristic
e	=	Eulerian
i	=	integral
m	=	maximum fE(f) or maximum u_u
d	=	diffuser
r	=	room

Superscripts

'	=	fluctuating component of quantity in question
^	=	estimated value

REFERENCES

Albright, L.D. 1989. Slotted inlet baffle control based on inlet jet momentum numbers. *Transactions of ASAE* 32(5):1764-1768.

Awbi, H.B. 1989. Application of computational fluid dynamics in room ventilation. *Building and Environment* 24(9):73-84.

Barber, E.M., and J.R. Ogilvie. 1982. Incomplete mixing in ventilated airspaces. Part I. Theoretical considerations. *Canadian Agricultural Engineering* 24(1):25-29.

Bodman, G.R. 1991. The pig environment: Design and construction. *Proceedings of Nebraska Whole Hog Days*, University of Nebraska, Lincoln, February 26, pp. 19-40.

Boon, C.R. 1978. Airflow patterns and temperature distribution in an experimental piggery. *Journal of Agricultural Engineering Research* 23:129-139.

Boon, C.R. 1982. The effect of air speed changes on the group postural behaviour of pigs. *Journal of Agricultural Engineering Research* 27:71-79.

Chen, Q., A. Moser, and A. Huber. 1990. Prediction of buoyant, turbulent flow by a low-Reynolds-number k-ε model. *ASHRAE Transactions* 96(1)564-573.

Choi, H.L., L.D. Albright, and M.B. Timmons. 1990. An application of the K-ε turbulence model to predict how a rectangular obstacle in a slot-ventilated enclosure affects air flow. *Transactions of ASAE* 33(1):274-281.

El-Telbany, M.M.M., M.R. Mokhtarzadeh-Dehghan, and A.J. Reynolds. 1985. Single-sided ventilation - Part I. The flow between a cavity and external air stream. *Building and Environment* 20(1):15-24.

Fanger, P.O., and C.J.K. Pedersen. 1977. Discomfort due to air velocities in spaces. Edité pour Institut International du Froid International Institute of Refrigeration, Paris, France.

Gosman, A.D., P.V. Nielsen, A. Restivo, and J.H. Whitelaw. 1980. The flow properties of rooms with small ventilation openings. *ASME Journal of Fluids Engineering* 102:316-323.

Haghighat. F., J.C.Y. Wang, and Z. Jiang. 1990. Three-dimensional analysis of airflow pattern and contaminant dispersion in a ventilated two-zone enclosure. *ASHRAE Transactions* 96(1):831-839.

Hanzawa, H., A.K. Melikov, and P.O. Fanger. 1987. Airflow characteristics in the occupied zone of ventilated spaces. *ASHRAE Transactions* 93(1):524-539.

Harrison, R.M., and R. Perry, eds. 1977. *Handbook of air pollution analysis*. New York: Chapman and Hall.

Hinze, J.O. 1975. *Turbulence*. New York: McGraw-Hill.

Jin, Y., and J.R. Ogilvie. 1990. Near floor air speeds from center slot air inlets in swine barns. ASAE Paper No. 90-4004. St. Joseph, MI:ASAE.

Jin, Y., and J.R. Ogilvie. 1991a. Airflow and drafts. ASAE Paper No. 91-4536. St. Joseph, MI:ASAE.

Jin, Y., and J.R. Ogilvie. 1991b. Floor air speeds in a slot ventilated room (isothermal). ASAE Paper No. 91-4559. St. Joseph, MI: ASAE.

Lay, R.M., and G.M. Bragg. 1988. Distribution of ventilation air—Measurement and spectral analysis by microcomputer. *Building and Environment* 23(3):203-213.

Leonard, J.J., and J.B. McQuitty. 1988. Air mixing in a mechanically ventilated room. *Canadian Agricultural Engineering* 30(1):185-189.

Ljungqvist, B. 1979. Some observations on the interaction between air movements and the dispersion of pollution. Document 8. Swedish Council for Building Research, Stockholm, Sweden.

Melikov, A.K., H. Hanzawa, and P.O. Fanger. 1988. Airflow characteristics in the occupied zone of heated spaces without mechanical ventilation. *ASHRAE Transactions* 94(1):52-70.

Melikov, A.K., G. Langkilde, and B. Derbiszewski. 1990. Airflow characteristics in the occupied zone of rooms with displacement ventilation. *ASHRAE Transactions* 96(1):555-563.

Melikov, A.K., and J.B. Nielsen. 1989. Local thermal discomfort due to draft and vertical temperature difference in rooms with displacement ventilation. *ASHRAE Transactions* 95(2):1050-1057.

Murakami, S., S. Kato, and Y. Suyama. 1988. Numerical and experimental study on turbulent diffusion fields in conventional flow type clean rooms. *ASHRAE Transactions* 94(2):469-493.

Nielsen, P.V., A. Restivo, and J.H. Whitelaw. 1978. The velocity characteristics of ventilated rooms. *ASME Journal of Fluids Engineering* 100:291-298.

Panofsky, H.A., and J.A. Dutton. 1984. *Atmospheric turbulence: models and methods for engineering applications*. New York: John Wiley and Sons.

Pasquill, F., and F.B. Smith. 1983. *Atmospheric diffusion*. New York: John Wiley and Sons.

Randall, J.M., and V.A. Battams. 1979. Stability criteria for airflow patterns in livestock buildings. *Journal of Agricultural Engineering Research* 24(4):361-374.

Siuma, D.L., and G.M. Bragg. 1986. Stochastic modelling of room air diffusion. *Ventilation '85*, pp. 121-135, Elsevier Science Publishers.

Thorshauge, J. 1982. Air-velocity fluctuations in the occupied zone of ventilated spaces. *ASHRAE Transactions* 88(2):753-764.

Zhang, J.S., L.L. Christianson, and G.L. Riskowski. 1991. Mean and turbulent flow characteristics of isothermal and non-isothermal ventilation flows. ASAE Paper No. 91-4535. St. Joseph, MI:ASAE.

Zhang, J.S., L.L. Christianson, and G.L. Riskowski. 1989. Regional airflow characteristics in a mechanically ventilated room under non-isothermal conditions. *ASHRAE Transactions* 96(1):751-759.

Zhang, J.S., L.L. Christianson, G.J. Wu, and G.L. Riskowski. 1992. Detailed measurements of room air distribution for evaluating numerical simulation models. *ASHRAE Transactions* 98(1):58-65.